DETERMINATION OF THE COEFFICIENT OF HYDRAULIC RESISTANCE WHEN USING ANTI-TURBULENCE ADDITIVES

•

Alexander Nikolaev[1], Andrey Goluntsov[1], Alberto Turro Breff[2]
Department of Transportation and Storage of Oil and Gas, St. Petersburg Mining University, RUSSIA
Ministry of Higher Education, CUBA
gas.ru@mail.com

Abstract

The article discusses rheological models of non-Newtonian oils, and also analyzes existing theories on reducing hydraulic resistance when using anti-turbulence additives, the main methods and approaches to transporting high-viscosity oil. High-viscosity oil from the North Komsomolskoye field, as well as anti-turbulence additives from the Monomer company, were used as the object of study. As a result of processing the results of experimental studies, the rheological model of oil was determined, and the effectiveness of using anti-turbulence additives from the Monomer company for this oil was established. The work also carried out a comparative analysis of the existing dependencies of the hydraulic resistance coefficient, compared the main dependencies and found that the most accurate models are those based on the universal law of resistance and the Altschul logarithmic formula, taking into account the Deborah number and the model for calculating efficiency through the value.

Keywords: highly viscous oil; heavy oil; additives; transport; coefficient of hydraulic resistance; reserves of high-viscosity oil; Toms effect.

I. Introduction

Currently, reserves of light, low-viscosity oil are being depleted. This fact poses an urgent task for companies in the fuel and energy complex involved in drilling wells, field development and transportation, to study and resolve the issue of the economic feasibility of using heavy, highly viscous oils. In practice, this issue is fraught with enormous technical difficulties, ranging from the extraction of such oil to its refining [45].

Transportation of high-viscosity oil is one of the key challenges facing the modern oil industry. Due to its special rheological properties, such oil creates serious difficulties for engineers and technologists: its viscosity makes it difficult to move through pipelines, increases energy costs for pumping and contributes to equipment wear [1-3].

Currently, there are several main methods of transporting non-Newtonian oils: “hot” pumping, electric heating, hydropumping of high-viscosity oil, transporting oil with diluents, adding depressants and anti-turbulence additives to oil. Currently, one of the developing methods of oil transport is the transport of oil with anti-turbulence additives. This type of additives allows you to reduce hydraulic resistance during fluid movement; they can significantly change the physical and chemical properties of oil, improving its fluidity and reducing viscosity.

The principle of operation of anti-turbulence additives is based on the Toms effect. The Toms effect was discovered in the 1940s and has since been widely used in the oil industry. The essence of this phenomenon is that when a small amount of polymers is added to a liquid, its flow becomes more orderly, which reduces friction and facilitates the movement of liquid through the pipeline. This is especially true for highly viscous oil, which, without the use of additives, moves with high energy consumption. Additives that cause the Toms effect facilitate its movement

through pipelines by changing the flow structure. As a result, the speed of oil movement increases and the energy consumption of the pumping process decreases.

The use of PTP also makes it possible to use the pipeline network more flexibly - to expand bottlenecks, replenish the volume of supplies after forced downtime, respond to changes in the viscosity of the pumped oil, to a shortage of electricity in a particular area, to changes in oil prices on the market.

The presence of turbulent flow is one of the necessary conditions for the operation of the PTP. Therefore, for heavy oils with high viscosity values, which are transported in laminar mode, the use of PTP will not lead to an increase in productivity. However, for oils with a viscosity of the order of several hundred centistokes, the use of PTP is possible; it is also possible to use PTP for heated oils or when pumping with a diluent, when a turbulent regime is realized.

Anti-turbulence additives can be divided into 3 types: polymers, fibers and surfactants.

The shares of drug consumption by region are distributed as follows: North America – 54.2%, Europe – 9.0%, Middle East – 13.1%, Southeast Asia – 4.4%, Africa – 11.7%, Countries CIS – 4.0%, China – 3.7%.

For the first time on an industrial scale, PTPs were tested in 1979 on the Trans-Alaska main oil pipeline with a diameter of 1219 mm by the company in order to increase the throughput of the oil pipeline. In 1978, TAPS conducted a very thorough laboratory study of the process of producing polymers in order to improve their characteristics. As a result, a polymer additive was developed, which was named CDR-101 and began to be used in the company's pipelines. In 1980, a number of changes were made to the polymerization process, which led to the creation of a new high-performance polymer additive CDR-102. Within two years of using CDR-102 additives from Conoco Specialty Products Inc, the pipeline capacity was increased from 16 to 32 thousand m^3/day [4-5].

The world's leading manufacturers, as a rule, have a wide range of additive brands designed for various types of pumped products. The main producers on the global DTP market (80-90%) are foreign companies ConocoPhillips (USA) and Baker Hughes (USA).

Based on the results achieved, these companies have developed a line of PTP specifically for heavy oil based on polar polymers that have the ability to dissolve in the presence of a high content of asphaltenes.

There are also several small producers on the market, for example, FlowChem (USA), Propipe (Spain, USA), Champion (UK, Netherlands) and the Chinese company China National Petroleum Co., which, as a rule, have a local business.

II. Materials and Methods

2.1. Reological models

Rheological models are used to describe the behavior of non-Newtonian fluids, that is, fluids whose dynamic (or effective) viscosity depends on shear stress and is not a constant value. Some of the most common rheological models for non-Newtonian fluids are: The Shvedov-Bingham model is used to describe liquids that have an initial yield strength τ0, below which it does not flow and has the properties of a solid.

The Shvedov-Bing equation has the form:

$$\tau = \tau_0 + \eta \cdot \dot{\gamma} \quad (1)$$

where τ - shear stress, η - viscosity coefficient, γ - shear rate.

The Ostwald-de Waele model is a generalization of Newton's law of viscosity and describes, for example, the flow of polymer solutions. In this model, viscosity varies proportionally to the degree of strain rate:

$$\tau = K \cdot \dot{\gamma}^n \quad (2)$$

where K - model parameter, n is an index that determines the degree of nonlinearity.

The Herschel-Bulkley model is used to describe thixotropic liquids. In this model, shear stress is represented by the equation:

$$\tau = \tau_0 + K \cdot \dot{\gamma}^n \quad (3)$$

The Casson model is used to describe pseudoplastic fluids, in which the viscosity decreases with increasing shear stress, and has the form:

$$\tau^{\frac{1}{2}} = \tau_c^{\frac{1}{2}} + \eta_c^{\frac{1}{2}} \cdot \dot{\gamma}^{\frac{1}{2}} \quad (4)$$

where $\tau_c^{\frac{1}{2}}$ is Casson yield stress, η_c is Casson plastic viscosity.

The Prandtl model is used to describe the behavior of viscoelastic materials and has the following form:

$$\tau = arscin\left(\frac{\dot{\gamma}}{B}\right) \quad (5)$$

The Cisco model is used as a rheological model of pseudoplastic fluids and has the form:

$$\tau = \eta_\infty \cdot \dot{\gamma} + \eta \cdot \dot{\gamma}^n \quad (6)$$

To take into account the nonlinearity of changes in shear stress with increasing shear rate in non-Newtonian fluids, Williamson and Gillespie proposed introducing a special correction factor:

$$\eta = \frac{\tau_0}{\dot{\gamma} + \chi} + \eta_\infty \quad (7)$$

The Cross model is considered a transformation of the previous model and is quite universal for describing the behavior of viscous liquids:

$$\eta = \frac{(\eta_0 - \eta_\infty)}{\left(1 + \frac{\dot{\gamma}}{\chi}\right)} + \eta_\infty \quad (8)$$

The Carreau model is used to describe the behavior of nonlinear viscous media in isothermal and non-isothermal processes and takes into account the thixotropic properties of the liquid being studied:

$$\eta = (\eta_0 - \eta_\infty)(1 + (\lambda\dot{\gamma})^2)^{\frac{n-1}{2}} + \eta_\infty \quad (9)$$

There is also a modified Carreau-Yasuda model, which is used to describe dispersed and polymer systems and has the form:

$$\eta = \frac{\tau_0}{(\dot{\gamma}^n + \chi)^m} + \eta_\infty \quad (10)$$

To describe a viscous liquid containing dispersed particles, the Ree-Eyring model is used:

$$\eta = (\eta_0 - \eta_\infty)\frac{arcsh(\beta\dot{\gamma})}{\beta\dot{\gamma}} + \eta_\infty \quad (11)$$

The Rayner-Rivlin model is used to describe a rheologically complex viscous fluid:

$$\dot{\gamma} = \sum_{n=0} a_{2n} \cdot \tau^{2n+1} \quad (12)$$

There are a large number of rheological models that describe the behavior of non-Newtonian fluids. By transforming some of them, it is possible to obtain others, but analysis shows that there is no universal way to describe the behavior of a non-Newtonian fluid.

2.2. Hypotheses about the mechanism for reducing hydraulic resistance when using polymer additives

Polymer additives are one of the most effective means of reducing hydraulic resistance when transporting high-viscosity oil. Currently, there are several main hypotheses explaining the mechanism of their action.

The first hypothesis suggests that the polymers form a thin layer on the inner walls of the pipeline that acts as a kind of “lubricant” reducing friction between the pipe walls and the flow of oil.

The second hypothesis is related to changes in the structure of oil flow under the influence of polymers. It is assumed that polymers are able to “destroy” turbulence in a flow, turning it from turbulent to laminar or transitional. This also leads to a reduction in friction and, accordingly, hydraulic resistance.

The third hypothesis is the possibility of changing the physical and chemical properties of the oil itself under the influence of polymers, which can lead to a change in its viscosity and density.

These hypotheses are not mutually exclusive and may operate simultaneously. Table 1 summarizes the above, as well as other existing hypotheses about the nature of the reduction in hydraulic resistance when using polymer additives. The hypotheses are grouped according to the key features of the proposed mechanism of resistance reduction.

Table 1: *Hypotheses about the mechanism for reducing hydraulic resistance when using polymer additives*

Theory	Brief description
Molecular stretch	Turbulent flow, mixing with the polymer, deforms it. The influence of polymers on viscosity is significant, so the vortex is damped. This leads to excess local viscosity and energy dissipation [6-8]. These ideas were developed in work, where the stretching of macromolecules is accompanied by an increase in rigidity in the direction of stretching, which leads, in turn, to a significant increase in longitudinal viscosity. As the longitudinal viscosity increases, the formation of large-scale vortices and emissions in the near-wall region is inhibited.
Reduced turbulence generation	Some researchers [9-11] believe that polymer additives prevent the onset of turbulence and the effect of reducing drag is associated not with the dissipation of vortex energy, but with the suppression of their generation. However, it is possible that both mechanisms take place simultaneously.
Reduced turbulent dissipation	Some researchers [12-15] believe that polymer additives prevent the onset of turbulence and the effect of reducing drag is associated not with the dissipation of vortex energy, but with the suppression of their generation. However, it is possible that both mechanisms take place simultaneously.
Vortex stretching	It is postulated that the tensile resistance of the vortices reduces mixing and energy loss. Dilute polymer solutions can have longitudinal viscosities that are up to a thousand times higher than the steady-state viscosities, which can influence the drag reduction mechanism. The authors of the work [16-18] believe that the destruction of the vortex occurs as a result of the destruction of macromolecules due to energy absorption.
Anisotropic properties and turbulence	In a turbulent flow regime, the additive polymers are stretched in the direction of the flow. Uneven absorption of flow energy occurs and leads to anisotropy of turbulent transfer. Viscosity increases as turbulent

	movement occurs along the normal to the wall of the pipes, and as a result, the intensity of velocity pulsations normal to the wall decreases [19-21].
Laminarization of turbulent flow	Turbulence involves the waste of energy through the formation of tiny vortices, which leads to increased drag. Therefore, the reduction in resistance is a measure of flow laminarization.
Pseudoplasticity	It is assumed that the near-wall layer, due to pseudoplasticity (a decrease in viscosity under the influence of shear), may have a lower friction coefficient than that of a pure solvent. The theory was not developed, since a decrease in viscosity under the influence of shear, although it occurs, is by a smaller amount than the decrease in resistance [22-25].
Viscoelasticity and normal stresses	Polymer solutions exhibit viscoelasticity and normal stress differences, but at concentrations much higher than those required to reduce resistance. Very dilute solutions have no measurable elasticity and do not differ in viscosity from pure solvents. On the other hand, viscoelastic solutions of chemically cross-linked polyacrylic acid do not exhibit a resistance-reducing effect, although they exhibit pseudoplasticity. Thus, viscoelasticity is not a necessary condition for drag reduction.
Formation of supramolecular agglomerates	This theory implies a decrease in resistance when conditions are realized in a turbulent flow for intermolecular interaction, while in a static state, dilute mixtures of polymers remain molecularly dispersed.

The presence of several theories indicates the absence of a single mechanism for reducing hydraulic resistance using anti-turbulence additives.

The lack of a unified theory entails different approaches to applied calculations for determining the Toms effect and calculating the efficiency of reducing hydraulic resistance (calculating the coefficient of hydraulic resistance when using PTP) depending on different flow conditions.

2.3 Analysis of dependencies to determine the coefficient of hydraulic resistance using PTP

In world practice, there are many different models for calculating the coefficient of hydraulic resistance in a mixture with additives and criteria describing the effectiveness of the additive.

However, most of them were derived from studying the Toms effect in aqueous solutions.

One of the main and classic universal models is the model proposed by A.D. Altshul [26-28]:

$$\frac{1}{\sqrt{\lambda}} = 1{,}8 \cdot \lg\left[\frac{Re_0}{Re_0 \frac{0{,}1 \cdot k_э}{D} + 7}\right] \quad (13)$$

where λ – coefficient of hydraulic resistance for flow using an additive; Re_0 is the Reynolds number without adding an additive.

Another model for calculating the hydraulic resistance coefficient using anti-turbulence additives in an oil flow is a model that takes into account the Deborah number:

$$\lambda = \frac{\lambda_0}{(1 + De^2)^m} \quad (14)$$

where m – the Leibenzone coefficient.

The Deborah number is determined by the following equation:

$$De = \alpha_0 \theta^{\alpha_1} Re_0^{\alpha_2} \quad (15)$$

where θ – additive concentration, g/t; α_0, α_1, α_2– empirical coefficients.

The Reynolds number in this case is:

$$Re = Re_0(1 + De^2) \quad (16)$$

In the work of the authors [29-32], based on experiments with additives, the following model for calculating the hydraulic resistance coefficient is proposed:

$$\lambda = 0{,}11\left(\frac{Z + \varepsilon + X^{1,4}}{115X + Y + 1}\right)^{0,25} \quad (17)$$

where ε – elative roughness of the inner surface of the pipe; $Z = \frac{68}{Re}$ – (Reynolds number used for flow using additive).

$$Y = A \cdot C^p \cdot \varepsilon^b \quad (18)$$

$$X = (28 \cdot Z)^{10} \quad (19)$$

A, p, b – constant coefficients for a certain additive.

The authors of works [33-37], based on the semi-empirical theory of turbulence by T. Karman, derived a universal equation for hydraulic flow resistance together with the use of anti-turbulence additives:

$$\frac{1}{\sqrt{\lambda}} = 0{,}88 \cdot ln \ln\left[\frac{k_1(C) Re\sqrt{\lambda}}{1 + 0{,}35k_2(C) \cdot \varepsilon \cdot Re\sqrt{\lambda}}\right] - 3{,}745 \quad (20)$$

The values of the coefficients $k_1(C)$ and $k_2(C)$ are determined during experiments with additives. It is allowed to take $k_2(C) = 0.32$.

In [38-41], a model based on the power formula of A.D. Altshul was proposed:

$$\lambda_f = \left[0{,}11 \cdot \left(\frac{68}{Re} + \varepsilon\right)^{0,25}\right] \cdot (1 + C)^{-0,25} \quad (21)$$

where $\varepsilon = \frac{k}{D}$ – roughness of the inner wall of the pipe surface; D - pipeline diameter, m; Re – Reynolds number for liquid flow with anti-turbulence additives; C – concentration of antihypertensive drugs

In [42-43], the theory of T. Karman was also taken as a basis and the following equation was obtained for finding the value of the coefficient of hydraulic resistance in a flow using additives:

$$\frac{1}{\sqrt{\lambda}} = 0{,}88 \cdot ln \ln\left[\mathrm{A} \cdot Re \cdot \sqrt{\lambda}\right] - 3{,}745 \quad (22)$$

where A is a coefficient that takes into account the interaction of turbulent flow with the pipe wall, equal to A=A0=28 in the absence of additive.

One of the well-known models describing the coefficient of hydraulic resistance is the Colebrook-White model based on pipe roughness:

$$\frac{1}{\sqrt{\lambda}} = -2 \cdot log \log\left(\frac{k}{3{,}7 \cdot D} + \frac{2{,}51}{Re \cdot \sqrt{\lambda}}\right) \quad (23)$$

where k – pipe roughness.

2.3. Experimental apparatus and procedure

When developing methods for studying high-viscosity oils and choosing instruments for their implementation, it is necessary to take into account the features of the multicomponent systems under consideration. Firstly, when they flow over smooth surfaces, the effect of wall sliding occurs due to a change in their properties near the solid surface. Secondly, the presence of thixotropic properties complicates their

experimental studies, since it is necessary to know and take into account the background of sample processing and the fact that the orientational thixotropic effect affects the rheological characteristics.

The essence of this effect is that, depending on the velocity field, one or another dynamically equilibrium state of the structure is created. The mutual orientation of particles ensures the predominance of a certain type of contact and interaction between them, which leads to a significant change in the properties of the original system. For experimental studies, oil from the North Komsomolskoye field was used.

Experimental studies were carried out using a rotational rheometer "Rheotest RN 4.1", widely used in the oil industry.

The general view of the rotational rheometer "Rheotest RN 4.1" is shown in Figure 1.

Figure 1. The general view of the rotational rheometer "Rheotest RN 4.1".

The main technical characteristics of the rotary viscometer "Rheotest RN 4.1" are given in Table 2.

Table 2: *The main technical characteristics of the rotary viscometer "Rheotest RN 4.1"*

Characteristics	Value
Dynamic viscosity measurement range, mPa·s	from 1 to 3.0·109
Limits of permissible relative error of the viscometer, %	±3
Number of measuring pairs, pcs.	17
Shear stress range, Pa	from 1.3 to 3.5·105
Range of shear rate gradients, s-1	from 0.04 to 20000
Temperature reading range, ℃	from -60 to +200
Smallest sample volume of the tested oil, ml	from 5 to 75 (depending on the measuring pair)

For experimental studies, oil from the Severo-Komsomolskoye oil field was used. The physical and chemical properties of oil are presented in Table 3.

Table 3: *The physical and chemical properties of oil*

Characteristics	Oil (20°C)
Density, kg/m3	945,5
Viscosity at 20°C, mm2/s	1216,2
Resin content, %	14,12
Paraffin content, %	0,62
Asphaltene content, %	1,02

At the beginning of the experiment, the oil sample is heated to the required temperature in a heating cabinet and then placed in a special cuvette of the device. After temperature control of the oil and parts of the device, the rotor is started, which begins to rotate with increasing angular velocity.

The friction force between the moving rotor and stationary oil causes the rotation of the rotor to accelerate or decelerate, which is monitored by the device's sensors. This change in rotation speed allows the dynamic viscosity of the sample to be determined.

It is important to note that measurements are carried out under strictly controlled conditions of temperature and pressure, as these parameters can significantly affect the results.

III. Results

During the experiment, graphs and values of shear stress and dynamic viscosity versus shear rate were obtained.

In Fig. 2-6 shows a graph of dynamic viscosity versus shear rate for pure oil from the North Komsomolskoye field.

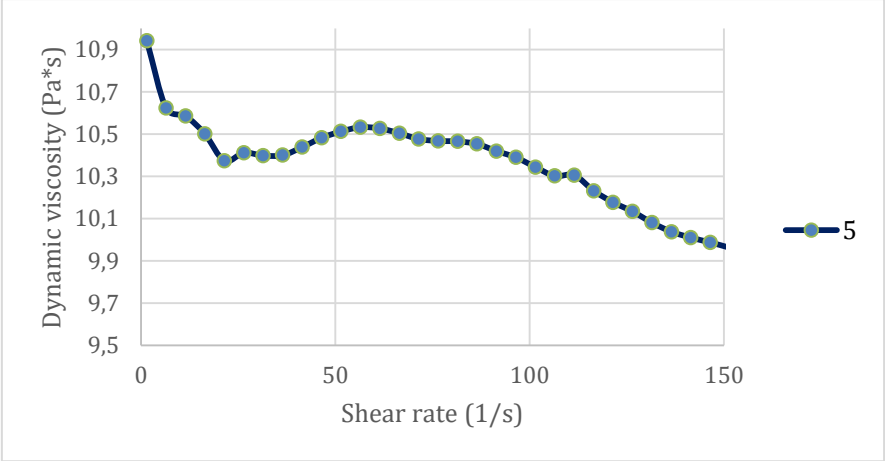

Figure 2: *Dynamic viscosity versus shear rate*

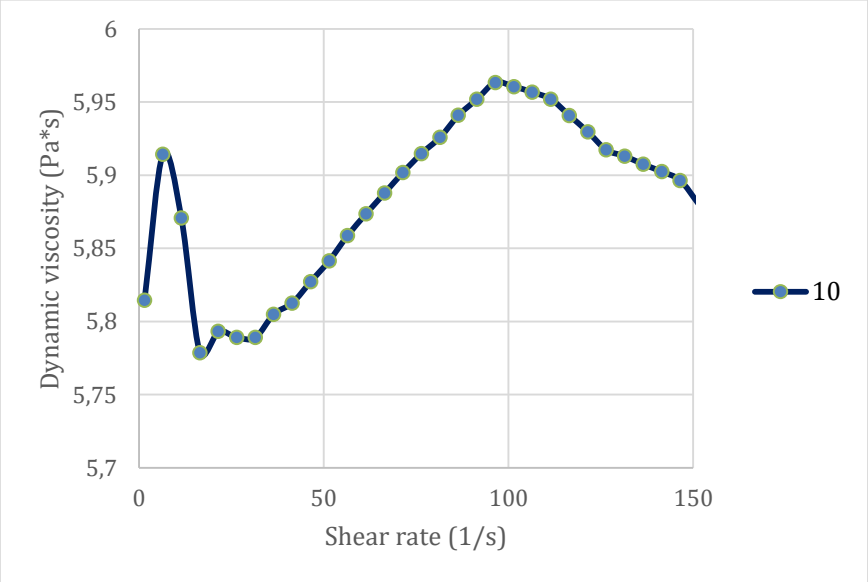

Figure 3: *Dynamic viscosity versus shear rate*

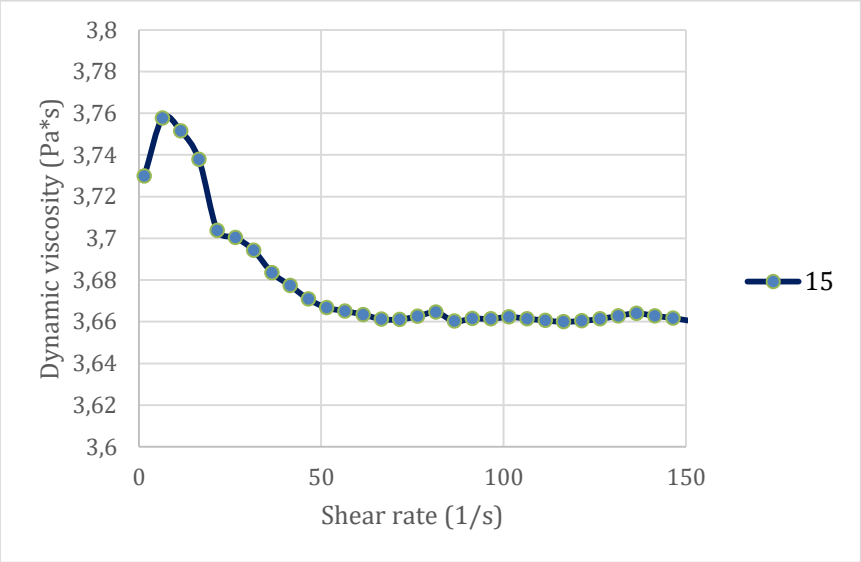

Figure 4: *Dynamic viscosity versus shear rate*

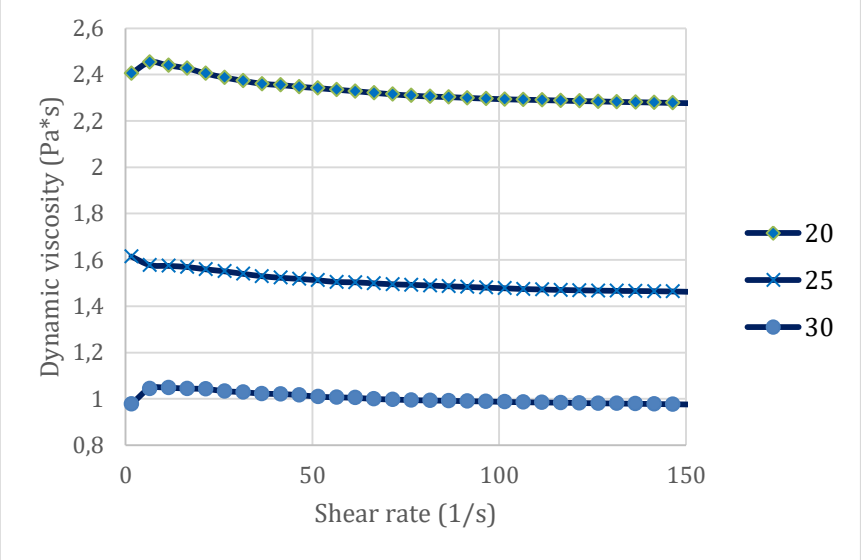

Figure 5: *Dynamic viscosity versus shear rate*

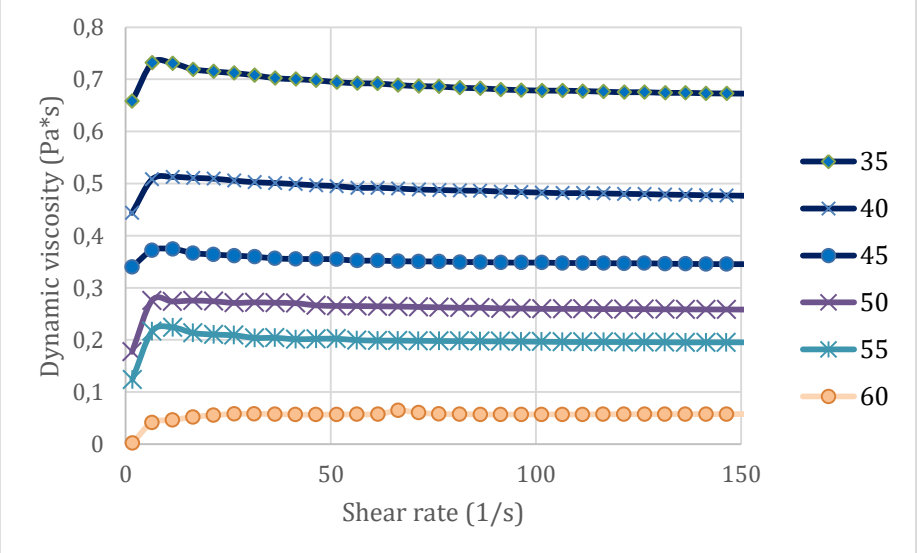

Figure 6: *Dynamic viscosity versus shear rate*

The graph shows that the oil begins to exhibit Newtonian properties in the temperature range from 40 to 45 °C (change in English version). The static shear stress at a temperature of 10 °C is 3.15 Pa (Remove).

The experimental results were processed using the least squares method. The resulting curves can be described by the nonlinear Bulkley-Herschel equation:

$$\tau = \tau_0 + k' \cdot \gamma^n \quad (24)$$

where τ_0 is the initial shear stress, k' is a coefficient depending on the consistency (the higher the viscosity, the greater k'), n is the index (depending on the shear rate).

Graphs describing the movement of liquid when adding an anti-turbulence additive at different temperatures are presented in Figure 7-10.

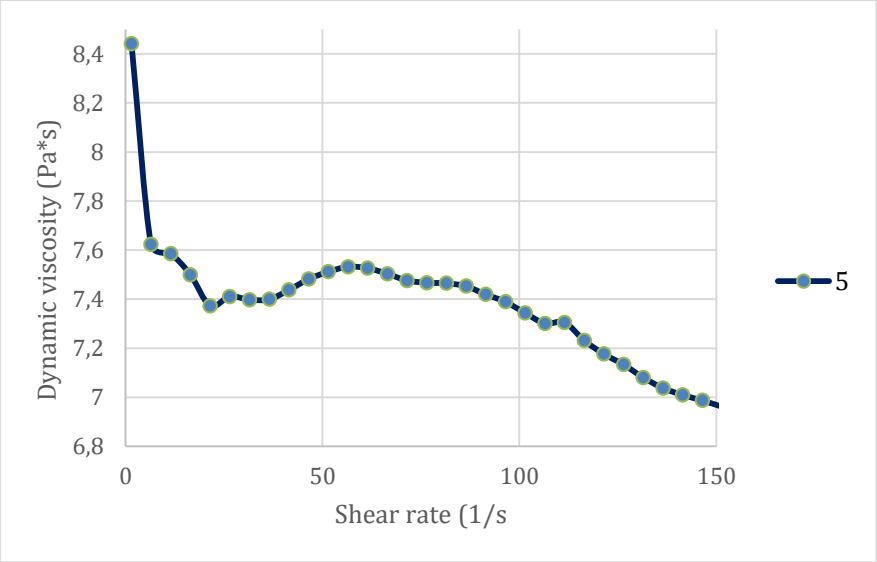

Figure 7: *Dynamic viscosity versus shear rate*

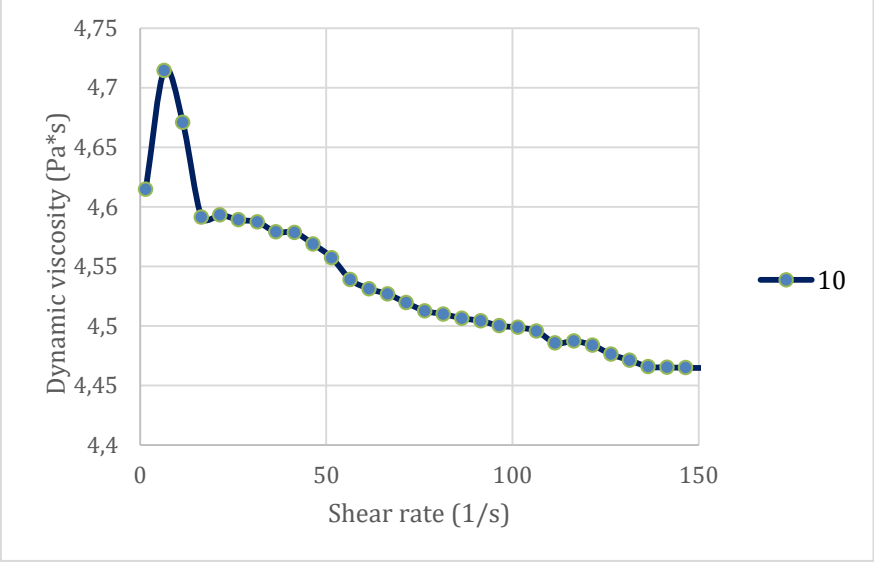

Figure 8: *Dynamic viscosity versus shear rate*

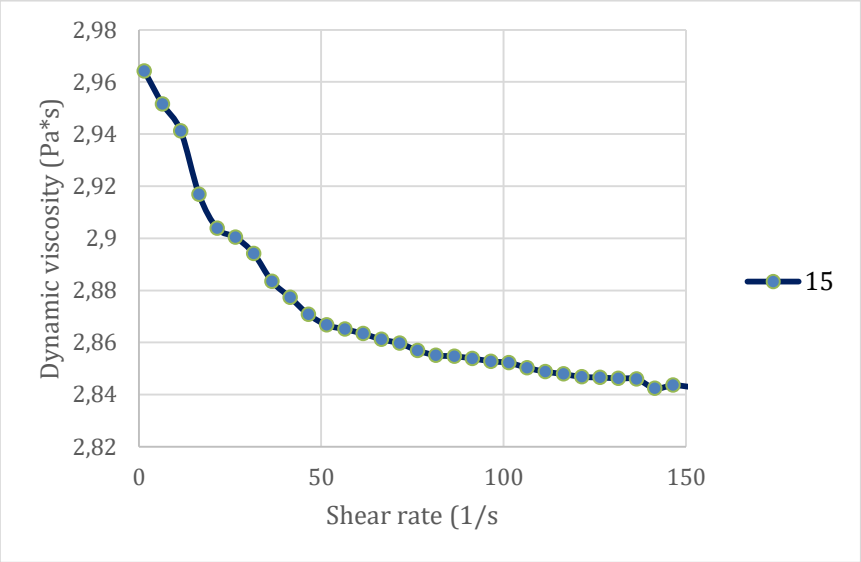

Figure 9: *Dynamic viscosity versus shear rate*

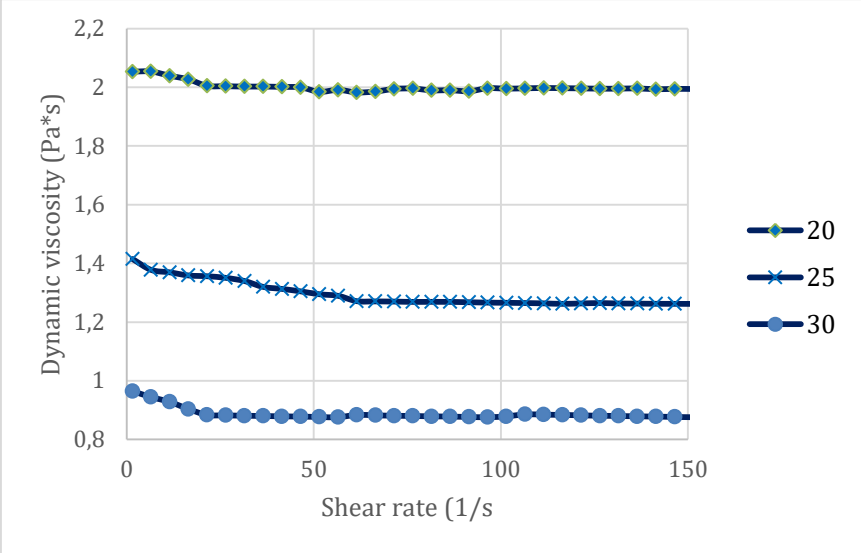

Figure 10: *Dynamic viscosity versus shear rate*

When transporting oil with an anti-turbulence additive, it is important to take into account the value of coefficient A1(0), which when transporting pure oil is a constant value, but when adding an additive changes its values and affects the value of the hydraulic resistance coefficient.

The results of determining the value of $A1(C)$ in modes using PTP are shown in Figure 12.

During the experiment, graphs and values of shear stress and dynamic viscosity from shear rate were obtained.

Figure 11 shows graph of the dependence of shear stress on shear rate.

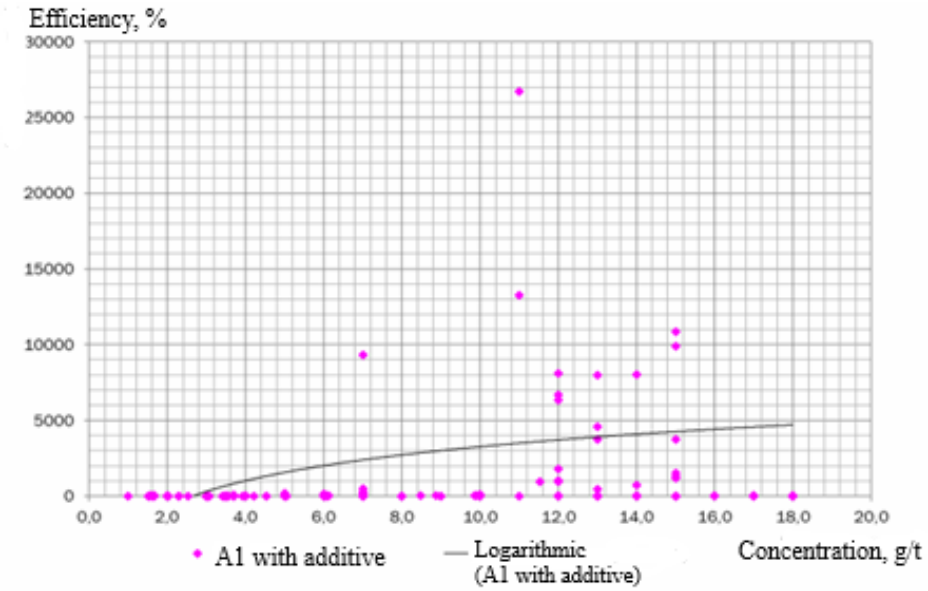

Figure 11: *Coefficient A1(C) in modes using PTP*

From Figure 11 it is clear that in modes with PTP the value of $A1(C)$ varies in a wide range from 1 to several 1000. Moreover, in contrast to the literature data from Figure 3.2 it is clear that the construction of any analytical dependence of the value of $A1(C)$ on concentration problematic. This indicates that the value of $A1$ is influenced not only by the concentration value, but also by a number of other factors.

To increase the accuracy of the calculation, the value of $A1$ was in the form $A1 = f\ (C, Re, \tau w)$. Based on the optimization results, a predictive calculation formula was constructed: $A1 = f\ (C, Re, \tau w)$, which gives the smallest error in determining the efficiency value ψQ. The results of comparison of actual efficiency values ψQ and calculated using the formula are presented:

$$\frac{1}{\sqrt{\lambda_f}} = 0{,}782 \cdot \ln\left(\left(1 + A_1(C, Re, \tau_w)\right) \cdot W_f\right) \quad (25)$$

From Figure 4 it can be seen that when applying the resulting formula, the convergence of the calculated data to the average efficiency values is quite good, however, some values related to high efficiencies above 60%, or low values obtained at high concentrations, differ from the calculated ones.

Based on the results of the analysis of actual and calculated values of efficiency ψQ when using the model under study, it was established that the average error is 10%.

The efficiency of PTP increases with increasing concentration of PTP in the pumped liquid; for the practical use of PTP on a specific pipeline, a curve of efficiency versus concentration ψ(C) is constructed, which is called the PTP efficiency curve. An example of this curve is shown in Figure 12.

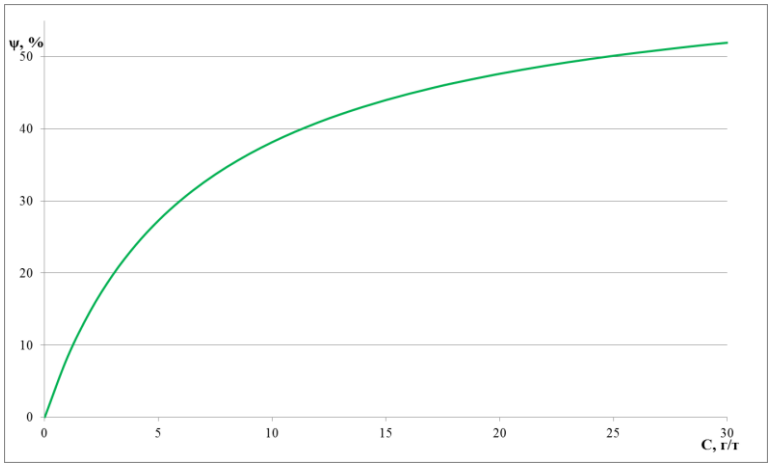

Figure 12: *DTP effectiveness curve*

The dependence of the effectiveness on the concentration of antipsychotic drugs, which quite accurately describes the behavior of antipsychotic drugs, can be presented in analytical form:

$$\frac{C}{\psi} = a + b \cdot C \tag{26}$$

Coefficients a, b are determined empirically, for example, as a result of pilot testing of PTP on a pipeline.

Based on the results of the research, a combined Q-H characteristic of pumping equipment and a section of the main pipeline with and without PTP was obtained, presented in Figure 13.

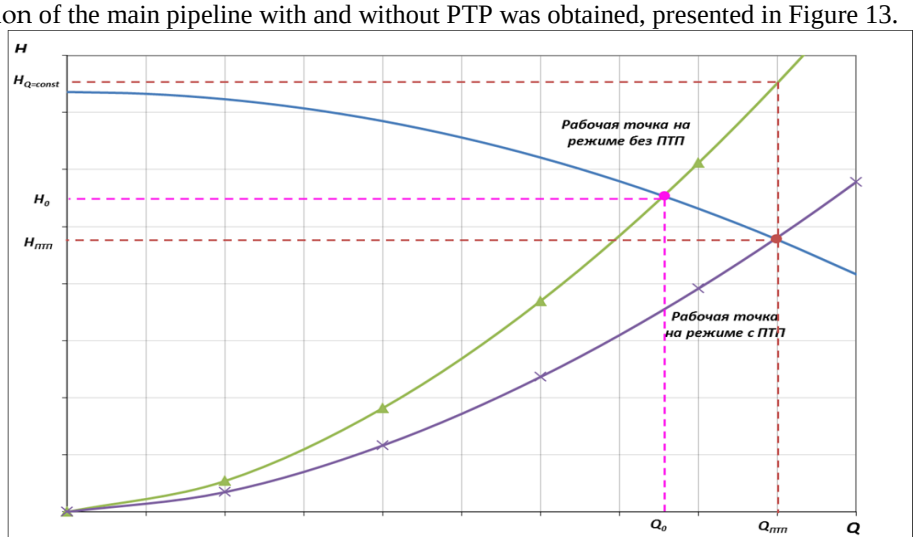

Figure 13: *Combined Q-H characteristics of pumping equipment and a section of the main pipeline with and without PTP*

In addition to the concentration of PRP, its effectiveness is influenced by a number of other factors: characteristics of the pipeline (pipeline length, its diameter, pipe wall roughness), properties of the pumped liquid (temperature, asphaltene content, solubility of PRP in the pumped liquid), flow regime (Reynolds number, shear stress on the wall of the pipeline), etc. [2].

Determination of hydraulic resistance based on the Colebrook-White equation for rough pipes:

$$\frac{1}{\sqrt{\lambda}} = 2 \cdot \log\left(\frac{Re \cdot \sqrt{\lambda}}{2{,}51} + N\right) \tag{27}$$

On the measuring line of the stand with diameter d1 and Reynolds number Re1, the value of $\frac{Re \cdot \sqrt{\lambda}}{2{,}51} + N$ is determined.

Next, the equation is solved for λ_1 for a pipeline with diameter d2:

$$\frac{1}{\sqrt{\lambda_2}} = 2 \cdot log\ \log\left(\frac{Re_1 \cdot \sqrt{\lambda_1}}{2{,}51} + N_1\right) \cdot \frac{d_2}{d_1}) \tag{28}$$

The Reynolds number corresponding to the found value of λ_2 is determined:

$$Re_2 = Re_1 \sqrt{\frac{\lambda_1}{\lambda_2}} \cdot \frac{d_2}{d_1} \quad (29)$$

This method, based on experimental studies on an installation with a Re1 number, makes it possible to predict the effectiveness of the ATA for a pipeline with a diameter of d2 and the Re2 number, which depends on the ratio of diameters, the coefficient of hydraulic resistance and the Re1 number.

Table 4: *Calculation results using the Colebrook-White model*

D, mm	Consumption, m3/h	Temperature, oC	Negative roughness	Deviation of hydraulic resistance,%
50	10	20	366,8	9,2
	20			2,5
	30			-2,5
	50			-1,9

3.2. Calculation of the hydraulic resistance coefficient based on the model with the Deborah number (14):

$$\lambda\lambda_P = \frac{\lambda_0}{(1 + De^2)^m}$$

Table 5: *Results of calculations using the model with the Deborah number*

D, mm	Consumption, m3/h	Temperature, oC	α_0	α_1	De	Deviation of hydraulic resistance,%
50	10	20	121,5	-0,5134	1,9	1,6
	20		121,5	-0,5134	1,2	-1,5
	30		121,5	-0,5134	0,9	1,5
	50		121,5	-0,5134	0,7	-0,9

3.3. Calculation of the hydraulic resistance coefficient based on a model that takes into account mixture formation (19):

$$\frac{1}{\sqrt{\lambda}} = 0{,}88 \cdot ln \ln\left[\frac{k_1(C) Re\sqrt{\lambda}}{1 + 0{,}35 k_2(C) \cdot \varepsilon \cdot Re\sqrt{\lambda}}\right] - 3{,}745$$

Results of calculation presented in Table 6.

Table 6: *Calculation results using a model that takes into account mixture formation*

D, mm	Consumption, m3/h	Temperature, oC	ε	k_1	k_2	Deviation of hydraulic resistance,%
50	10	20	0,00184	56	0,31	6,1
	20		0,00184	56	0,31	3,1
	30		0,00184	56	0,31	-2,9
	50		0,00184	56	0,31	-2,1

3.4. Calculation of the hydraulic resistance coefficient based on the T. Karman model using the transcendental equation (21):

$$\frac{1}{\sqrt{\lambda}} = 0{,}88 \cdot ln \ln\left[\mathrm{A} \cdot Re \cdot \sqrt{\lambda}\right] - 3{,}745$$

Results of calculation presented in table 7.

Table 7: *Results of calculations using the T. Karman model*

D, mm	Consumption, m3/h	Temperature, oC	A	Deviation of hydraulic resistance,%
50	10	20	41,2	9,9
	20		41,2	10,1
	30		41,2	-5,4
	50		41,2	-7,2

3.5. Calculation of the coefficient of hydraulic resistance based on the model of the universal law of resistance and Altschul's logarithmic formula:

$$\frac{1}{\sqrt{\lambda_f}} = 0{,}782 \cdot ln\ \ln\left[A_1 \cdot W_f\right] \quad (30)$$

where λ_f – coefficient of hydraulic resistance using ATA; $A_1(C)$ - coefficient depending on the concentration of the additive.

$$W_f = \frac{Re_f}{Re_f \cdot \frac{0{,}1 \cdot k_e}{D} + 7} \quad (31)$$

where k_e – roughness, Re_f – Reynolds number with ATA.

Table 8: *Results of calculations using the model based on the universal law of resistance and Altschul's logarithmic formula*

D, mm	Consumption, m3/h	Temperature, oC	A_1	W_f	Deviation of hydraulic resistance,%
50	10	20	1,1	406,8	6,1
	20		1,1	798,2	3,2
	30		1,1	1410,2	-2,5
	50		1,1	1850,2	-2,3

Models based on the universal law of resistance and the Altschul logarithmic formula, taking into account the Deborah number, and a model for calculating efficiency through the value of Re on the installation and the real pipeline turned out to be more accurate.

IV. Conclusions

As a result of the research, the following results were obtained:

1. Oil from the North Komsomolskoye field corresponds to the Bulkley-Herschel model and exhibits non-Newtonian properties in the temperature range from 10 to 20 degrees

2. A comparison of models of the hydraulic resistance coefficient showed that for a given type of oil the universal law of resistance and the Altschul logarithmic formula, taking into account the Deborah number and a model for calculating efficiency through the value of Re on the installation and the real pipeline.

Acknowledgments: The authors gratefully acknowledge the support of the Department of Transport and Storage of Oil and Gas, Saint Petersburg Mining University.

References

[1] Zakirova, G; Pshenin, V; Tashbulatov, R; Rozanova, L. Modern Bitumen Oil Mixture Models in Ashalchinsky Field with Low-Viscosity Solvent at Various Temperatures and Solvent Concentrations. Energies. 2023; 16(1):395. https://doi.org/10.3390/en16010395.

[2] Aleksander G., P., Yifan, T., & Fuming, Z. (2023). Predicting Service Life of Polyethylene Pipes under Crack Expansion using "Random Forest" Method. International Journal of Engineering, 36(12), 2243-2252. https://doi.org/10.5829/ije.2023.36.12c.14

[3] Nikolaev, A.; Plotnikova, K. Study of the Rheological Properties and Flow Process of High-Viscosity Oil Using Depressant Additives. Energies 2023, 16, 6296. https://doi.org/10.3390/en16176296.

[4] Palaev G., A., Fuming, Z., & Yifan, T. (2024). Method for Assessing Damage to Gas Distribution Network Pipelines based on Nonlinear Guided Wave. International Journal of Engineering, 37(5), 852-859. https://doi.org/10.5829/ije.2024.37.05b.04

[5] Shagiev, R.G.; Gumerov, A.G.; Khudyakova, L.P. The problem of degradation of anti-turbulent additives in pipelines of hydrocarbon raw materials. Sci. Technol. Pipeline Transp. Oil Oil Prod. 2017, 11, 41–47.

[6] Zhang, L.; Du, C.; Wang, H.; Zhao, J. Three-dimensional numerical simulation of heat transfer and flow of waxy crude oil in inclined pipe. Case Stud. Therm. Eng. 2022, 37 102237.

[7] Fetisov, V. Analysis of numerical modeling of steady-state modes of methane–hydrogen mixture transportation through a compressor station to reduce CO2 emissions. Sci Rep 14, 10605 (2024). https://doi.org/10.1038/s41598-024-61361-3

[8] Kumar, R.; Banerjee, S.; Mandal, A.; Naiya, T.K. Flow improvement of heavy crude oil through pipelines using surfactant extracted from soapnuts. J. Pet. Sci. Eng. 2017, 152, 353–360. https://doi.org/10.1016/j.petrol.2017.02.010.

[9] Ghoneim, N.I.; Megahed, A.M. Numerical Analysis of the Mixed Flow of a Non-Newtonian Fluid over a Stretching Sheet with Thermal Radiation. Fluid Dyn. Mater. Process. 2023, 19, 407–419.

[10] Shammazov I.A., Borisov A.V., Nikitina V.S. Modeling the Operation of Gravity Sections of an Oil Pipeline. Bezopasnost Truda v Promyshlennosti // Occupational Safety in Industry. 2024. № 1. pp. 74–80. (In Russ.). DOI: 10.24000/0409-2961-2024-1-74-808

[11] Mukhaimer, A.; Al-Sarkhi, A.; El Nakla, M.; Ahmed, W.; Al-Hadhrami, L. Pressure drop and flow pattern of oil–water flow for low viscosity oils: Role of mixture viscosity. Int. J. Multiph. Flow 2015, 73, 90–96. https://doi.org/10.1016/j.ijmultiphaseflow.2015.02.018.

[12] Mardashov, D.V.; Bondarenko, V.; Raupov, I.R. Technique for calculating technological parameters of non-Newtonian liquids injection into oil well during workover. J. Min. Inst. 2022, 254, 1–14.

[13] Wang, K.; Wang, Z.M.; Song, G.-L. Batch transportation of oil and water for reducing pipeline corrosion. J. Pet. Sci. Eng. 2020, 195, 107583. https://doi.org/10.1016/j.petrol.2020.107583.

[14] Bolobov, V.; Martynenko, Y.; Yurtaev, S. Experimental Determination of the Flow Coefficient for a Constrictor Nozzle with a Critical Outflow of Gas. Fluids 2023, 8, 169. https://doi.org/10.3390/fluids8060169

[15] X. Luo, G. Lü, W. Zhang, L. He, Y. Lü. Flow structure and pressure gradient of extra heavy crude oil-water two-phase flow. J. Exp. Therm. Fluid Sci., 82 (2017), pp. 174-181, doi.org/10.1016/j.expthermflusci.2016.11.015.

[16] Ulyasheva, N.; Leusheva, E.; Galishin, R. Development of the drilling mud composition for directional wellbore drilling considering rheological parameters of the fluid. J. Min. Inst. 2020, 244, 454–461. https://doi.org/10.31897/pmi.2020.4.8.

[17] J. Shi, M. Gourma, H. yeung. CFD simulation of horizontal oil-water flow with matched density and medium viscosity ratio in different flow regimes. J. J. Petrol. Sci. Eng., 151 (2017), pp. 373-383, doi.org/0.1016/j.petrol.2017.01.022.

[18] Perveitalov, O.G.; Nosov, V.V.; Schipachev, A.M.; Alekhin, A.I. Thermally Activated Crack Growth and Fracture Toughness Evaluation of Pipeline Steels Using Acoustic Emission. Metals 2023, 13, 1272. https://doi.org/10.3390/ met13071272

[19] Schipachev, A.; Aljadly, M.; Ganzulenko, O.; Chernikov, D.; Razzhivin, V.; Yusupov, R. Evaluating the Effectiveness of Magnetic-Pulse Treatment for Healing Continuity Defects in the Metal of Oil and Gas Pipelines. Metals 2023, 13, 1875. https://doi.org/10.3390/met13111875

[20] Lorena A. dos Santos, Danielda C. Ribeiro, Oldrich J.Romero. Heavy oil transportation through steam heating: An analytical and numerical approach. Journal of Petroleum Science and Engineering Volume 195, December 2020, 107932, doi.org/10.1016/j.petrol.2020.107932.

[21] Qian Huang, Hongying Li, Yu Zhuang, Yifei Ding, Chenbo Ma, Chaohui Chen, Yiwei Xie, Huaqing Liang, Shanpeng Han, Jinjun Zhang. Reducing viscosity of waxy crude oil with electric field perpendicular to oil's flow direction. Fuel Volume 283, 1 January 2021, 119345, doi.org/10.1016/j.fuel.2020.119345.

[22] Xiaoqing Li, Renqiang Liu, Hui Jiang, Peng Yu, Xiaoyan Liu. Numerical investigation on the melting characteristics of wax for the safe and energy-efficiency transportation of crude oil pipelines. Measurement: Sensors Volumes 10–12, 15 November 2020, 100022, doi.org/10.1016/j.measen.2020.100022.

[23] P. Babakhani, A. Azdarpour, E. Mohammadian. The hydrodynamic behavior of high viscous oil-water flow through horizontal pipe undergoing sudden expansion-CFD study and experimental validation. Chem. Eng. Res. Des., 139 (2018), pp. 144-161, doi.org/10.1016/j.cherd.2018.09.026.

[24] A. Archibong-Eso, J. Shi, Y.D. Baba, A.M. Aliyu, Y.O. Raji, H. Yeung. High viscous oil-water two-phase flow: experiments & numerical simulations. Heat Mass Tran., 55 (3) (2019), pp. 755-767, doi.org/10.1007/s00231-018-2461-9.

[25] J. Shi, M. Gourma, H. Yeung. CFD simulation of horizontal oil-water flow with matched density and medium viscosity ratio in different flow regimes. J. Petrol. Sci. Eng., 151 (2017), pp. 373-383, doi.org/10.1016/j.petrol.2017.01.022.

[26] Nikolaev, A., Lykov, Y.V., Duchnevich, L. (2018). Mathematical modeling of non-stationary gas flow in gas pipeline. IOP Conference Series: Materials Science and Engineering, 327. 327 (2), pp.1-6. https://doi.org/10.1088/1757-899X/327/2/022034

[27] Palaev A. G., Nosov V. V., Krasnikov A. A. Simulating distribution of temperature fields and stresses in welded joint using ANSYS. Science & Technologies: Oil and Oil Products Pipeline Transportation. 2022;12(5):461–469. https://doi.org/10.28999/2541-9595-2022-12-5-461-469

[28] Mingyan Shao, Palaev Aleksander, Yuhong Xia, Huiying Xu, Yifan Tian, Vadim Fetisov, A.M. Shipachev, Zhenqing Yang, Understanding the phase behavior during CO2 flooding by dissipative particle dynamics, Journal of Molecular Liquids, Volume 409, 2024, 125514, ISSN 0167-7322, https://doi.org/10.1016/j.molliq.2024.125514

[29] Xiaoqing Li, Renqiang Liu, Hui Jiang, Peng Yu, Xiaoyan Liu. Numerical investigation on the melting characteristics of wax for the safe and energy-efficiency transportation of crude oil pipelines. Measurement: Sensors Volumes 10–12, 15 November 2020, 100022, doi.org/10.1016/j.measen.2020.100022

[30] P.Babakhani, A. Azdarpour, E. Mohammadian. The hydrodynamic behavior of high viscous oil-water flow through horizontal pipe undergoing sudden expansion-CFD study and experimental validation. Chem. Eng. Res. Des., 139 (2018), pp. 144-161, doi.org/10.1016/j.cherd.2018.09.026

[31] A. Archibong-Eso, J. Shi, Y.D. Baba, A.M. Aliyu, Y.O. Raji, H. Yeung. High viscous oil-water two-phase flow: experiments & numerical simulations. Heat Mass Tran., 55 (3) (2019), pp. 755-767, doi.org/10.1007/s00231-018-2461-9

[32] Sultanbekov, R.R.; Schipachev, A.M. Manifestation of incompatibility of marine residual fuels: a method for determining compatibility, studying composition of fuels and sediment. J. Min. Inst. 2022, 257, 843–852.

[33] J. Shi, M. Gourma, H. Yeung. CFD simulation of horizontal oil-water flow with matched density and medium viscosity ratio in different flow regimes. J. Petrol. Sci. Eng., 151 (2017), pp. 373-383, doi.org/10.1016/j.petrol.2017.01.022

[34] Samigullin G H , Schipachev A. M., Samigullina L. G., Fetisov V. G. Assessment of damage of metallic elements in oil and gas facilities using small punch test International Journal of Applied Engineering Research. 2017. №12. pp. 11583-11587.

[35] Rafael Martínez-Palou, María de Lourdes Mosqueira, Beatriz Zapata-Rendón, Elizabeth Mar-Juárez, César Bernal-Huicochea, Juande la Cruz Clavel-López, Jorge Aburto. Transportation of heavy and extra-heavy crude oil by pipeline: A review. Journal of Petroleum Science and Engineering Volume 75, Issues 3–4, January 2011, pp. 274-282, doi.org/10.1016/j.petrol.2010.11.020

[36] Litvinenko, V.S.; Tsvetkov, P.S.; Dvoynikov, M.V.; Buslaev, G.V. Barriers to implementation of hydrogen initiatives in the context of global energy sustainable development. J. Min. Inst. 2020, 244, 428–438.

[37] N.H.Abdurahman, Y.M.Rosli, N.H.Azhar, B.A.Hayder. Pipeline transportation of viscous crudes as concentrated oil-in-water emulsions. Journal of Petroleum Science and Engineering Volumes 90–91, July 2012, pp. 139-144, doi.org/10.1016/j.petrol.2012.04.025

[38] Xintong Huang, Cuihong Zhou, Quanyu Suo, Lanting Zhang, Shihan Wang. Experimental study on viscosity reduction for residual oil by ultrasonic. Ultrasonics Sonochemistry Volume 41, March 2018, pp. 661-669, doi.org/10.1016/j.ultsonch.2017.09.021

[39] Wanqing Wang, Chenxi Yi, Wu. Xiaochuan, et al. Heavy oil viscosity reduction methods overview Sichuan Chem. Ind., 2 (2013), pp. 13-17, doi.org/10.4028/www.scientific.net/AMR.602-604.13

[40] Fetisov, V.G., Nikolaev, A., Lykov, Y.V. (2017). Experimental Studies for Determining Gas Flow Rate Accidental Release on Linear Part of Pipeline, 87 (6), pp.1-9. https://doi.org/10.1088/1755-1315/87/6/062003

[41] Korobov, G. Y., Vorontsov, A. A., Buslaev, G. V, and Nguyen, V. T. "Analysis of Nucleation Time of Gas Hydrates in Presence of Paraffin During Mechanized Oil Production." International Journal of Engineering, Vol. 37, No. 7, (2024), 1343–1356. https://doi.org/10.5829/ije.2024.37.07a.13

[42] C.A.M. Cavicchio, J.L. Biazussi, M.S. de Castro, A.C. Bannwart, O.M.H. Rodriguez, C.H.M. de Carvalho. Experimental study of viscosity effects on heavy crude oil-water core-annular flow pattern. J. Exp. Therm. Fluid Sci., 92 (2018), pp. 270-285, doi.org/10.1016/j.expthermflusci.2017.11.027

[43] X. Luo, G. Lü, W. Zhang, L. He, Y. Lü. Flow structure and pressure gradient of extra heavy crude oil-water two-phase flow. J. Exp. Therm. Fluid Sci., 82 (2017), pp. 174-181, doi.org/10.1016/j.expthermflusci.2016.11.015

[44] Mardashov, D.V. Development of blocking compositions with a bridging agent for oil well killing in conditions of abnormally low formation pressure and carbonate reservoir rocks. J. Min. Inst. 2021, 251, 617–626. https://doi.org/10.31897/PMI.2021

[45] Nasibova G. J. et. al., (2023). Oil and gas prospects of tectonic crashing zones of the Kura intermountain depression. "Reliability: Theory and Applications" RT&A, 5 (75), Volume 18, 313-322. https://doi.org/10.24412/1932-2321-2023-575-313-322.